

We are IntechOpen, the world's leading publisher of Open Access books Built by scientists, for scientists

4,800

Open access books available

122,000

International authors and editors

135M

Downloads

Our authors are among the

154

Countries delivered to

TOP 1%

most cited scientists

12.2%

Contributors from top 500 universities



WEB OF SCIENCE™

Selection of our books indexed in the Book Citation Index
in Web of Science™ Core Collection (BKCI)

Interested in publishing with us?
Contact book.department@intechopen.com

Numbers displayed above are based on latest data collected.

For more information visit www.intechopen.com



Lattice Boltzmann Computations of Transport Processes in Complex Hydrodynamics Systems

Zhiqiang Dong¹, Weizhong Li², Yongchen Song² and Fangming Jiang¹

¹CAS Key Laboratory of Renewable Energy and Gas Hydrate, Guangzhou Institute of Energy Conversion, Chinese Academy of Sciences, Guangzhou

²Key Laboratory of Ocean Energy Utilization and Energy Conservation of Ministry of Education, Dalian University of Technology, Dalian
China

1. Introduction

Lattice Boltzmann method (LBM) has recently been receiving considerable attention as a possible alternative to conventional computational fluid dynamics (CFD) approaches in many areas related to complex fluid flows. It is of great promise for simulating flows in topologically complicated geometries, such as those encountered in porous media, and for simulations of multi-component and/or multiphase flow conjugated with heat and mass transfer. In these particular areas, there are few viable conventional CFD methods for using. The present chapter deals with LBM numerical investigation to heat and mass transfer in flows with multiple components and/or phases encountered in the rotating packed-bed or nucleate pool boiling.

In the following section 2 the LB multi-component model is adapted for simulating the mixing process in a rotating packed-bed with a serial competitive reaction ($A+B\rightarrow R$, $B+R\rightarrow S$; A, B, R, and S denote different components.) occurred inside. The serial competitive reaction in the main filling area of a rotating packed-bed is simulated and the mass transfer with forced convection caused by a cylindrical filler (to mimic the packing material) is studied as well. The obtained results provide some guidance for further studying the forced mass-transfer in and for the design of the real rotating packed-bed in industries.

In section 3, a hybrid LBM model is constructed. In combination with a lattice Boltzmann thermal model, the lattice Boltzmann multiphase model being capable of handling a large density ratio between phases is extended to describe the phenomenon of phase change with mass and heat transferring through the interface. Based on the Stefan boundary condition, the phase change is considered as change of the phase order parameter and is treated as a source term in the Cahn-Hilliard(C-H) equation. The evolution of the interfacial position is thereby tracked. With an improved Briant's treatment to the partial wetting boundaries, this hybrid model is used to simulate the growth of a single vapour bubble on and its departure from a heated wall. Numerical results exhibit similar parametric dependence of the bubble departure diameter in comparison with the experimental correlation available in recent literatures. Furthermore, parametric studies on the growth, coalescence and departure of a pair of twin-bubbles on a heated wall are conducted as well.

2. LBM mass transfer model

In practical engineering, the fluid flow is commonly multiphase and/or multi-component flow. The interface between phases or components changes randomly with time and the boundary surfaces between fluid and solid are sometimes very topologically-complicate. These factors make the corresponding numerical study being of great challenge. Based on the lattice gas method (Frish et al., 1986) since 1992, LBM has been developed and employed in the area of computational fluid dynamics, particularly, for the simulations of multi-component flows. Alexander et al. (1993) first used the LBM work to study component delivery problems, but the model was limited to a fixed Prandtl number. Chen et al. (1997) introduced a matrix instead of the Bhatnagar-Gross-Krook (BGK) collision factor to overcome this limitation, but their method is subjected to some computational instability (Soe et al., 1998; Vahala et al., 1998; Vahala et al., 2000). Bartoloni et al. (1993) and Shan (1997) employed two distribution functions to enhance the stability of the calculation. Inamuro et al. (2002) further simplified the distribution function. Because non-linear first-order error term presents in the macroscopic diffusion equation, the LBM multi-component model has only first-order accuracy.

Via comparison with the analytical solution, this section firstly analyzes the truncation error and accuracy of LBM. Secondly, we build up the serial competitive reaction LBM and use this model to simulate the mass transfer process in a rotating packed-bed.

In a rotating packed bed, the extremely high rotation speed forms super large centrifugal body force, which can be hundreds times of the gravity. Multiphase and/or multi-component fluids flowing inside the porous packed-bed will be torn into micro- or even nano- sized fragments, leading to greatly elongated interfaces between phases or components and hence making the mixing process around 1 - 3 orders of magnitude more efficient than in the traditional mixing towers. In this section, mixing process with a serial competitive reaction in a simplified rotating packed-bed will be simulated using an improved LBM mass transport model.

2.1 Mathematical formulation and model validation

2.1.1 Mathematical formulation

Continuity and Navier-Stokes equations

We assume the fluid system contains fluid phase of n-components. The D2Q9 BGK model is applied and the equilibrium distribution function (f) of component n is formulated as follows,

$$f_a^{eq}(\mathbf{x}, t, n) = c_n \omega_a \left(1 + 3\mathbf{e}_a \cdot \mathbf{u} + \frac{9}{2}(\mathbf{e}_a \cdot \mathbf{u})^2 - \frac{3}{2}u^2 \right) \quad (1)$$

The term on the left hand side denotes the probability that component n is present at position \mathbf{x} , at time t along the direction a . The \mathbf{e}_a is the particle velocity, $e_0=0$; $e=\Delta\mathbf{x}/\Delta t$, $\Delta\mathbf{x}$

is the space step, Δt is the time step, $\omega_a = \begin{cases} 4/9, & a=0; \\ 1/9, & a=1,3,5,7; \\ 1/36, & a=2,4,6,8. \end{cases}$ c_n is the concentration of

component n, \mathbf{u} is the velocity vector of fluid flow. The corresponding LBM equation of component n is

$$f_a(\mathbf{x} + \mathbf{e}_a \varepsilon, t + \varepsilon, n) - f_a^{eq}(\mathbf{x}, t, n) = -\frac{f_a(\mathbf{x}, t, n) - f_a^{eq}(\mathbf{x}, t, n)}{\tau} \quad (2)$$

with τ being the relaxation parameter and ε the time step. We define the macroscopic variables as

$$c_n = \sum_a f_a^{eq}(\mathbf{x}, t, n) \tag{3}$$

$$c_n \mathbf{u}_i = \sum_a \mathbf{e}_{ia} f_a = \sum_a \mathbf{e}_{ia} f_a^{eq} \tag{4}$$

$$c(\mathbf{x}, t) = \sum_n c_n(\mathbf{x}, t, n) \tag{5}$$

By virtue of the Chapman-Enskog expansion and multiscale analysis, the corresponding continuity and Navier-Stokes equations yield

$$\frac{\partial c}{\partial t} + \frac{\partial c u_j}{\partial x_j} = 0 \tag{6}$$

$$\frac{\partial c u_i}{\partial t} + \frac{\partial c u_i u_j}{\partial x_j} = -\frac{\partial p \delta_{ij}}{\partial x_j} + \mu \frac{\partial^2 c u_i}{\partial x_j \partial x_j} + \eta \frac{\partial^2 c u_k}{\partial x_k \partial x_i} + o(\varepsilon^2) \tag{7}$$

where, the viscosity is calculated with $\mu=(2\tau-1)\varepsilon/6.0=\eta/2.0$, the pressure $\mathbf{p}=c/3$. Eqs. (6) and (7) ensure the multi-component system being of the general flow characteristics.

Mass transport equations of fluid components

Applying the Taylor series expansion and using the Chapman-Enskog approximation to Eq. (2), we get the following second order LB mass transport equation,

$$\frac{\partial}{\partial t} \sum_\alpha f_\alpha^{(0)} + \frac{\partial}{\partial x_i} \sum_\alpha \mathbf{e}_{i\alpha} f_\alpha^{(0)} + \varepsilon \left(\frac{1}{2} - \tau \right) \sum_\alpha \left(\frac{\partial}{\partial t_0} + \mathbf{e}_{i\alpha} \frac{\partial}{\partial x_i} \right)^2 f_\alpha^{(0)} + o(\varepsilon^2) = 0 \tag{8}$$

Combined with Eqs.(3)and (4), Eq.(8) can be expressed as

$$\frac{\partial c_n}{\partial t} + \frac{\partial c_n u_i}{\partial x_i} = \mu \frac{\partial^2 c_n}{\partial x_i^2} + \mu \frac{\partial^2 c_n u_i}{\partial t \partial x_i} + o(\varepsilon^2) \tag{9}$$

where, $\mu=(2\tau-1)\varepsilon/6.0$ is the diffusion coefficient. A perturbation term $\mu \frac{\partial^2 c_n u_i}{\partial t \partial x_i}$ of first-order

accuracy is present in the convection-diffusion equation. The dimensionless velocity u is very small, so the perturbation term only has little influence on the precision of Eq. (9). The difference between LBM and the traditional convection-diffusion equation is that the series truncation error term appears in the diffusion term of the corresponding macroscopic equation (9). This section focuses firstly on the truncation error term and the perturbation term to investigate their influence on the LBM diffusion behavior.

Mass transport with serial competitive reaction

We consider a serial competitive reaction: $A+B \rightarrow R ; B+R \rightarrow S$. The corresponding convection -diffusion equation is formulated as

$$\frac{\partial c_n}{\partial t} + \frac{\partial c_n u_i}{\partial x_i} = D \frac{\partial^2 c_n}{\partial x_i^2} - r_i \quad (10)$$

where, u_i is the x_i -direction velocity; c_n is the concentration of component n ; D is molecular diffusion coefficient; r_i is the source or sink term due to chemical reaction.

$$\begin{aligned} r_A &= k_1 c_A c_B \\ r_B &= k_1 c_A c_B + k_2 c_B c_R \\ r_R &= -k_1 c_A c_B + k_2 c_B c_R \\ r_S &= -k_2 c_B c_R \end{aligned} \quad (11)$$

where, k_1 and k_2 are rate constants.

Based on D2Q9 BGK model, the equilibrium distribution function of component n is set as follows.

$$f_a^{eq}(\mathbf{r}, t, n) = c_n \omega_a (1 + 3\mathbf{e}_a \cdot \mathbf{u} + \frac{9}{2}(\mathbf{e}_a \cdot \mathbf{u})^2 - \frac{3}{2}\mathbf{u}^2) \quad (12)$$

$$\mathbf{e}_a = e \left[\mathbf{i} \cos \frac{(\alpha - 1)}{2} + \mathbf{j} \sin \frac{(\alpha - 1)}{2} \right] \quad (13)$$

where, $1 \leq \alpha \leq 4$, $\mathbf{e}_0 = 0$, $\omega_a = \begin{cases} 4/9, & a = 0; \\ 1/9, & a = 1, 3, 5, 7; \\ 1/36, & a = 2, 4, 6, 8. \end{cases}$ \mathbf{i} , \mathbf{j} are the unit vector in the x , y direction,

respectively; \mathbf{e}_a is the particle velocity. The distribution function $f_a^{eq}(\mathbf{r}, t, n)$ denotes the mass fraction probability of component n presented at location \mathbf{r} , at time t and along the a direction. Using r_{na} to denote the corresponding chemical reaction term, the equation of LBM is thus obtained as

$$f_a(\mathbf{r} + \mathbf{e}_a \varepsilon, t + \varepsilon, n) - f_a^{eq}(\mathbf{r}, t, n) = -\frac{f_a(\mathbf{r}, t, n) - f_a^{eq}(\mathbf{r}, t, n)}{\tau} + r_{na} \quad (14)$$

Likewise, we define macroscopic variables:

$$\text{The node mass fraction of the component } \mathbf{n}: c_n = \sum_a f_a^{eq}(\mathbf{r}, t, n) \quad (15)$$

$$\text{The total mass fraction of nodes: } c(\mathbf{r}, t) = \sum_n c_n(\mathbf{r}, t, n) \quad (16)$$

$$\text{Node momentum of component } \mathbf{n}: \mathbf{c}\mathbf{u} = \sum_a \mathbf{e}_a \sum_n f_a(\mathbf{r}, t, n) = \sum_a \mathbf{e}_a \sum_n f_a^{eq}(\mathbf{r}, t, n) \quad (17)$$

$$\text{Node chemical reaction term of composition } \mathbf{n}: r_n = \sum_a r_{na} \quad (18)$$

Applying the Taylor series expansion and Chapman-Enskog expansion to Eq. (14), we can get a different time scale LBM equation. Bonded with the multi-scale equations, the following equation yields

$$\frac{\partial}{\partial t} \sum_{\alpha} f_{\alpha}^{(0)} + \frac{\partial}{\partial r} \sum_{\alpha} \mathbf{e}_{\alpha} f_{\alpha}^{(0)} + \varepsilon \left(\frac{1}{2} - \tau\right) \sum_{\alpha} \left(\frac{\partial}{\partial t_0} + \mathbf{e}_{\alpha} \frac{\partial}{\partial r}\right)^2 f_{\alpha}^{(0)} - \sum_{\alpha} r_{na} + o(\varepsilon^2) \tag{19}$$

Introducing Eqs. (15), (16), (17) and (18) into the Eq. (19), we get

$$\frac{\partial c_n}{\partial t} + \frac{\partial c_n u_i}{\partial x_i} = D \frac{\partial^2 c_n}{\partial x_i^2} - r_i + o(\varepsilon^2) \tag{20}$$

where, $D=(\tau-0.5)\varepsilon/3$ is the diffusion coefficient.

2.1.2 Model validation

In order to validate the model prediction we consider a transient diffusion case, which is described with:

$$\frac{\partial c}{\partial t} = \kappa \frac{\partial^2 c}{\partial x^2}, 0 < x < 1, t > 0 \tag{21}$$

The boundary and initial conditions are,

$$c(0,t) = 1, \frac{\partial c(1,t)}{\partial x} = 0, (t > 0); c(x,0) = 0, (0 \leq x \leq 1) \tag{22}$$

It has an analytical solution,

$$c(x,t) = 1 - \sum_{j=0}^{\infty} \frac{4}{(2j-1)\pi} \exp\left[-\frac{1}{4}\pi^2(j-1)^2 \kappa t\right] \sin\left[\frac{1}{2}\pi(2j-1)x\right] \tag{23}$$

As shown by Fig. 1, the LBM simulated results are in good agreement with the analytical solutions. No initial value fluctuation occurs in the LBM computation.

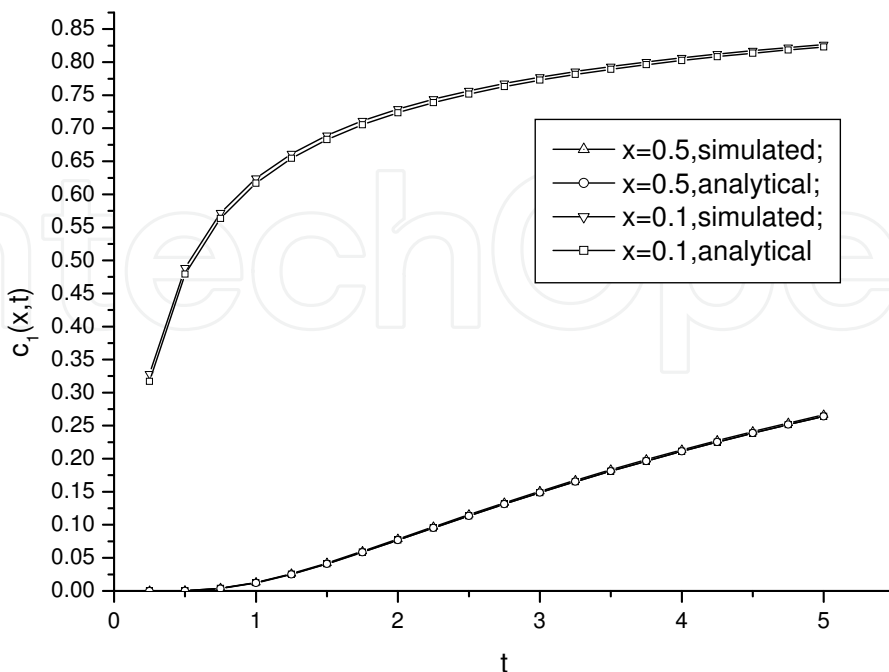


Fig. 1. Diffusion behavior without convection effect

The above test case verifies that the perturbation term $\mu \frac{\partial^2 c_n u_i}{\partial t \partial x_i}$ in Eq. (9) can be safely omitted. Hereby we validate the reliability and accuracy of the LBM diffusion transport model.

2.2 Mixing process with serial competitive reaction

2.2.1 Laminar diffusion and reaction model

Experimental results of TV camera image and stroboscopic photography show that the liquid flow in rotating packed-bed is mainly in the form of film flow (Liu, 2000). Due to the strong centrifugal force, the liquid film is very thin, thinner than tens of microns. Therefore, the Reynolds number is small (approximately less than 30) and thus the liquid flow falls in the laminar flow regime. To this understanding, we perform the LB modeling to the laminar diffusion and reaction process.

We consider a case that two liquid films meet and bond together and then move at the same speed with no tangential movement due to shear force. The diffusion is across the interface of two liquid films and the reaction is added: $A+B \rightarrow R$; $B+R \rightarrow S$. Analyzing this serial competitive reaction and comparing the first product R and second product S, we can quantify the reactive mass transport.

Fig.2 displays the concentration profile of each component of reactants and products, at position $i=75$ and at time $t=50000$ time steps, which corroborates the process follows the laminar diffusion and reaction regime. More simulation results about temporal variation of the total amount of each component ($c = \sum_{i,j} c(i,j)$) are shown in Fig. 3.

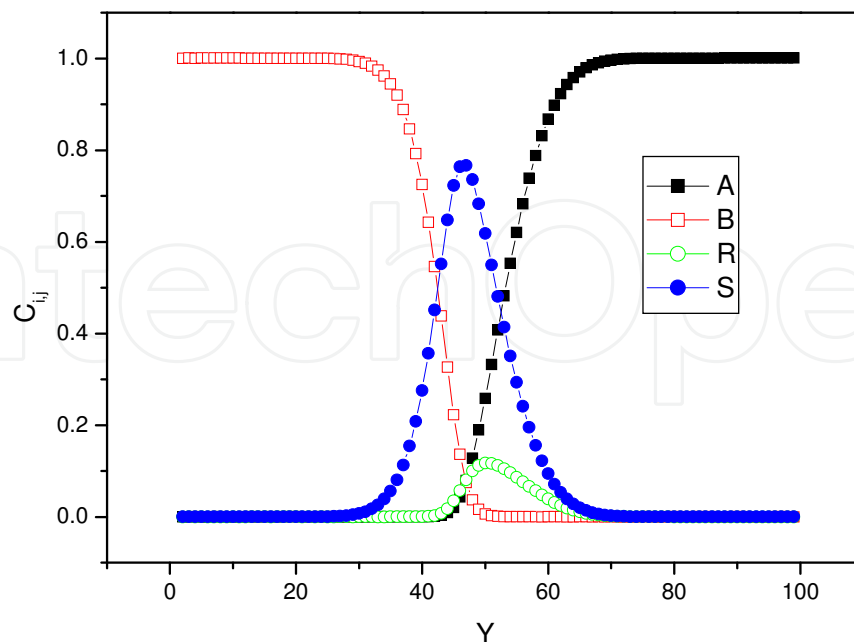


Fig. 2. Component concentration at $i=75$ and at $t=50000$ time steps

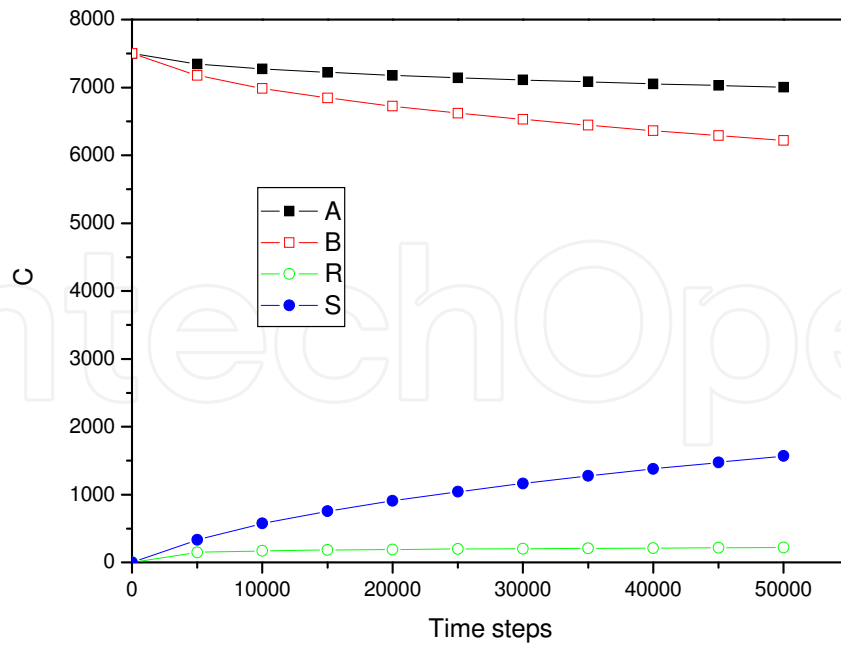


Fig. 3. Temporal variation of the total amount of each component

2.2.2 Forced convection and reaction model

To introduce convection disturbance to the mixing process, a cylindrical pillar is put at the entry section of the simulated geometry. The cylindrical pillar mimics one packed-filler in a rotating packed-bed. With the LBM, the mixing with serial competitive reaction at the end-effect regions of the rotating packed-bed is simulated and some hints about the convective mixing in the packed-bed are obtained. Typical results are shown in Figs. 4 and 5. The inserted pillar induces disturbance to fluid flow, deforming the interface of different components and hence enhancing the mixing process.

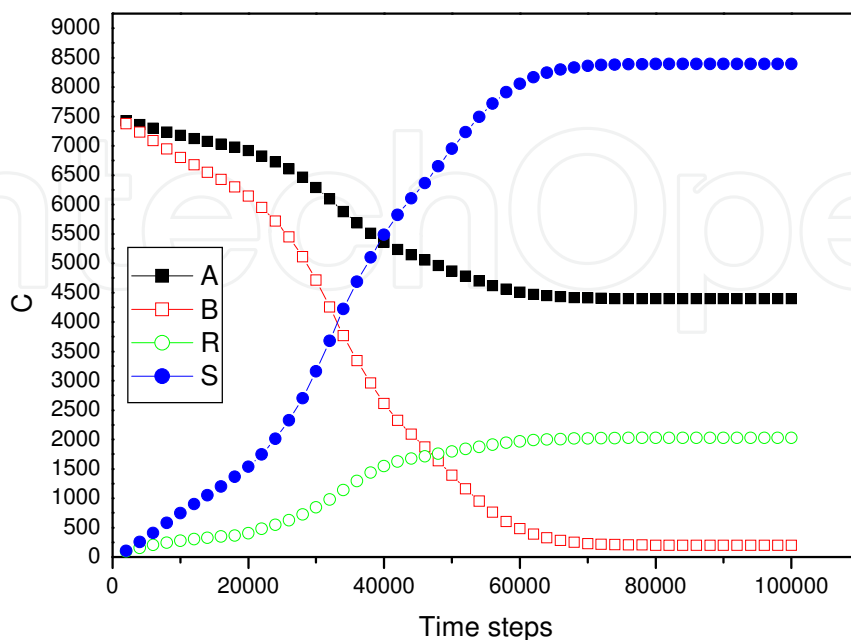
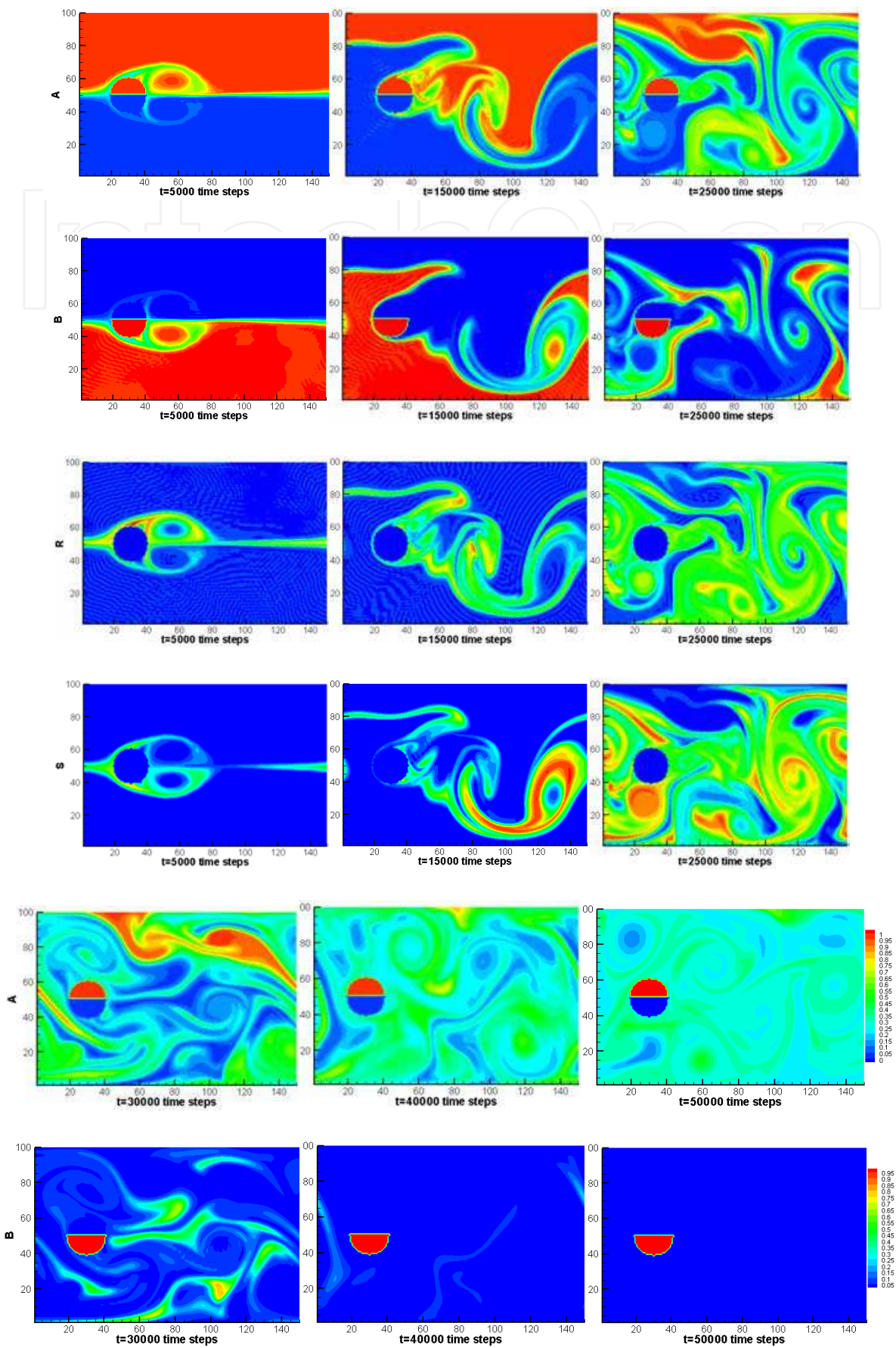


Fig. 4. Temporal variation of the total amount of each component



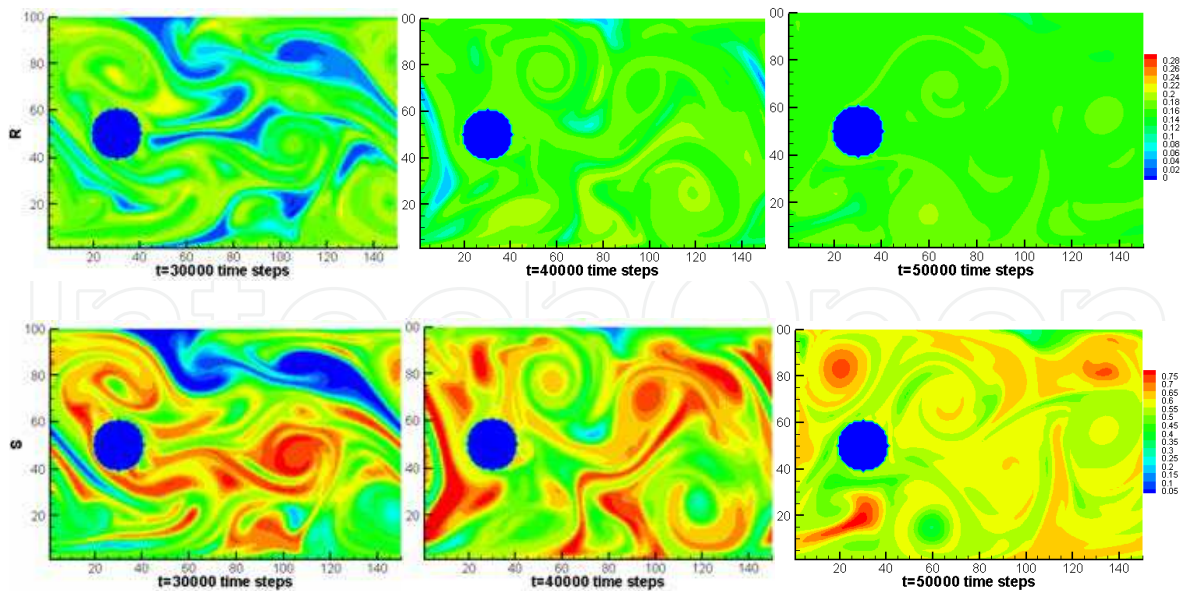


Fig. 5. Evolution of 2-D distribution of the reactant/product concentration

3. A hybrid lattice Boltzmann model

Nucleate boiling is a liquid-vapor phase-change process accompanying with the bubble formation, growth, departure and rising. Because the process plays a key role in the boiling heat transfer, it has been widely studied for half a century. Although the phenomenon of bubble motion with bubble growth can be explained qualitatively as demonstrated in the corresponding experimental investigations, main difficulty in quantitative prediction is that multiphase flows pose to be very complex, involving thermodynamics (co-existing phase), kinetics (nucleation, phase transitions) and hydrodynamics (inertial effects). "What role does a liquid-vapor interface play?" remains to be a core and open issue from the physical point of view. Fortunately, the development of numerical methods and computer technology has provided a powerful tool to predict vapor bubble behavior in nucleate pool boiling. For vapor bubble with phase-change, the vapor-liquid interface becomes extraordinary complicated because of its nonlinearity, variety, and time-dependence behavior induced by phase-change accompanying with heat and mass transfer. Therefore, treatment of the interface is a key problem in the simulation of multiphase flows including bubbly flows. Generally, numerical simulation of bubbly flows can be classified as: the singular interface model and the diffuse interface model. Earlier studies on vapor bubble dynamics were based on the Rayleigh equation and its modification, which were basically related to dealing with zero or one dimensional problems (Plesset & Zwick, 1953). Wittke & Chao (1967) studied the collapse of a spherical bubble with translatory motion. Cao & Christensen (2000) simulated the bubble collapse in a binary solution, in which the Navier-Stokes equation was transformed into the form of the stream function and vorticity in two-dimensional axisymmetric non-orthogonal body-fitted coordinates. Yan & Li (2006) simulated a vapor bubble growth as it rises in uniformly superheated liquid by using two numerical methods based on moving non-orthogonal body-fitted coordinates proposed by Li & Yan (2002a,2002b). Han et al. (2001) used a mesh-free method to simulate bubble deformation and growth in nucleate boiling. Fujita & Bai (1998) used the arbitrary Lagrange-

Eulerian (ALE) method to simulate the growth of a single bubble attached at a horizontal surface with a constant contact angle before its departure. These numerical simulations are the singular interface model, in which the grid is limited so as not to be fit to bubble large deformation in topology, such as coalescence and breakup of the bubble. In such a situation, the diffuse interface model, such as VOF (volume of fluid), the level set and phase field method etc., was proposed to recover the defects of the first kind of model. Tomiyama et al. (1993) simulated a single bubble by using the VOF. Hua & Lou (2007) developed the front tracking method to simulate the bubble rising in the quiescent viscous liquid due to buoyancy. Little progress had been made in the numerical simulation of bubbly flows with phase change based on the diffuse interface model. Son et al. (1998) simulated a growing and departing bubble on a horizontal surface and captured the vapor-liquid interface by the level set method which was modified to include the action of phase change. Ni et al. (2005) simulated the bubbly flows with phase change by the level set method as stated in Son et al. (1998)'s work. In their work, $\nabla \cdot u$ is applied to define the phase change and the interfacial velocity need to be separately obtained from the temperature condition at the interface. Nevertheless, little information in the literatures was reported about the vapor bubbles' behavior with phase change. In particular, few papers have been reported on the propagations of temperature field around a growing and deforming vapor bubble. Due to the complexity of environment about the realistic bubble flow like porous media, the treatment of boundary usually encounters a lot of embarrassment for the above-described methods. This point has limited and weakened the ability of these numerical methods to some extent.

Recently, the lattice Boltzmann method (LBM) became a popular tool to simulate the incompressible viscous flows due to its merits like the ease of boundary treatment and the parallel implementation. In the LB context, there were several models developed for multiphase and multi-component flows in the past two decades. The earlier works were the color method proposed by Rothman & Keller (1998), the potential method by Shan et al. (1993), the free energy method by Swift et al. (1996) and the method by He et al. (1999). These models have not been used in solving practical problems due to the limit of smaller density ratio between phases. Up to 2007, three models of large density ratio were proposed, the first one was an immiscible incompressible two-phase model with large density ratio proposed by Inamuro et al. (2004), the second one was that of Lee et al. (2005) and the third one was proposed by Zheng et al. (2006). Inamuro et al. (2004)'s model was used to track the two-phase interface by applying a diffuse equation which is analogy to the C-H equation. This kind of interface-tracking technique has the same principle as the level set method. In fact, the two-phase interface is also disposed as an index such as 0 and 1. Unlike Inamuro et al. (2004)'s and Lee et al. (2005)'s models, Zheng et al. (2006) approximated the C-H equation to track and define the two-phase interface without the artificial disposal adopted by other models in the physical background. Benefiting from the concept of the order parameter continuum in phase-change process following the regime of Landau mean-field theory, Zheng et al. (2006)'s model can be extended to non-isothermal systems with phase-change. Therefore, we proposed a hybrid LBM model (Dong et al., 2009), which is a combination of the Zheng et al. (2006)'s multiphase model and a thermal LBM model (Inamuro et al. 2002) and is able to characterize the heat and mass transfer in multiphase flows. In this hybrid model, Zheng et al. (2006)'s model is added with a source term to the corresponding C-H equation to define the phase-change and the thermal LBM model is added by a source term to define the latent heat. The modified C-H equation has a much clearer physical

explanation to the treatment of phase change at the interface, thus enabling to track the interface automatically by following the change of the phase order parameter.

3.1 Zheng’s lattice Boltzmann dynamic model

In the simulation of vapor bubbly flows, the binary model proposed by Zheng et al.(2006) is employed to track the dynamic evolution of the flow field. In Zheng et al. (2006)’s model, there are two independent macroscopic parameters, total number density, $n=(\rho_A+\rho_B)/2$ and number density difference, $\Phi=(\rho_A-\rho_B)/2$, where ρ_A and ρ_B stand for the density of fluid A and fluid B, respectively. The parameter n is proportional to pressure and approximately constant in the whole flow field. The parameter Φ becomes positive in the region where $\rho_A > \rho_B$ and negative in the region with $\rho_A < \rho_B$, and thus it represents two-phase distribution, which is the same as the definition in the Swift et al. (1996)’s model.

Two sets of discretized distribution functions f_i and g_i are used to assign each site, which are related to the parameters n and Φ , respectively. The distribution function f_i can be used to model the transport of mass and momentum, while the distribution function g_i can be employed to track the interface. Thus, the corresponding LB BKG equation is written as follows,

$$f_i(x + e_i\Delta t, t + \Delta t) - f_i(x, t) = \Omega_i \tag{24}$$

with

$$\begin{aligned} \Omega_i &= \frac{1}{\tau_n} [f_i(x, t) - f_i^{eq}(x, t)] + \left(1 - \frac{1}{2\tau_n}\right) \frac{\omega_i}{c_s^2} \left[(e_i - u) + \frac{(e_i \cdot u)}{c_s^2} e_i \right] (\mu\phi\nabla\phi + F_b) \delta t \\ g_i(x + e_i\Delta t, t + \Delta t) - g_i(x, t) &= (1 - q) [g_i(x + e_i\Delta t, t) - g_i(x, t)] \\ &\quad - \frac{1}{\tau_\phi} [g_i(x, t) - g_i^{eq}(x, t)] \end{aligned} \tag{25}$$

where, x is restricted to sites on the lattice and t is the discrete time, τ_n, τ_ϕ is the dimensionless relaxation parameter. The equilibrium distribution functions to satisfy the conservation laws can be expressed as follows:

$$n = \sum_i f_i^{(eq)} \tag{26}$$

$$u = \frac{1}{n} \left[\sum_i f_i^{(eq)} e_i + \frac{1}{2} (\mu\phi\nabla\phi + F_b) \right] \tag{27}$$

$$\sum_i f_i^{(eq)} e_{i\alpha} e_{i\beta} = (\phi\mu_\phi + c_s^2 n) \delta_{\alpha\beta} + nu_\alpha u_\beta \tag{28}$$

$$\sum_i g_i = \sum_i g_i^{(eq)} = \phi \tag{29}$$

$$\sum_i g_i^{(eq)} e_{i\alpha} = \frac{\phi}{q} u_\alpha \quad \text{with} \quad q = \frac{1}{\tau_\phi + 0.5} \tag{30}$$

$$\sum_i g_i^{(eq1)} e_{i\alpha} e_{i\beta} = \Xi_{\alpha\beta} \quad \text{with} \quad \Xi_{\alpha\beta} = \Gamma \mu_\phi \delta_{\alpha\beta} \quad (31)$$

where, u is the macroscopic velocity of the fluid. The chemical potential is given by:

$$\mu_\phi = A \left(4\phi^3 - 4\phi^2 \cdot \phi \right) - K \nabla^2 \phi \quad (32)$$

By performing a Chapman-Enskog expansion to Eqs. (24) and (25), the macroscopic equations for n and ϕ in the second order precision can be derived as follows.

$$\frac{\partial n}{\partial t} + \nabla \cdot (nu) = 0 \quad (33)$$

$$\frac{\partial (nu)}{\partial t} + \nabla \cdot (nuu) = -\nabla \cdot (P + \phi \mu_\phi) + \phi \nabla \mu_\phi + \nu \nabla^2 (nu) + F_b \quad (34)$$

$$\frac{\partial \phi}{\partial t} + \nabla \cdot (\phi u) = \theta_M \nabla^2 \mu_\phi \quad (35)$$

where, $\theta_M = q(\tau_\phi q - 0.5) \delta \Gamma$.

From Eqs. (33), (34) and (35), the corresponding equilibrium distribution functions can be constructed as follows:

$$f_i^{(eq)} = \omega_i A_i + \omega_i n \left(3e_{i\alpha} u_\alpha - \frac{3}{2} u^2 + \frac{9}{2} u_\alpha u_\beta e_{i\alpha} e_{i\beta} \right) \quad (\text{Based on D2Q9}) \quad (36)$$

$$\text{where } A_1 = \frac{9}{4} n - \frac{15 \left(\phi \mu_\phi + \frac{1}{3} n \right)}{4} \quad A_{i(i=2, \dots, 9)} = 3 \left(\phi \mu_\phi + \frac{1}{3} n \right),$$

$$\omega_1 = \frac{4}{9}, \omega_{i(i=2, \dots, 5)} = \frac{1}{9}, \omega_{i(i=6, \dots, 9)} = \frac{1}{36}.$$

$$g_i^{(eq)} = A_i + B_i \phi + C_i \phi e_i \cdot u \quad (\text{Based on D2Q5}) \quad (37)$$

where $B_1 = 1$, $B_i = 0 (i \neq 1)$, $C_i = \frac{1}{2q}$, $A_1 = -2\Gamma \mu_\phi$, Γ is the diffusion coefficient.

3.2 Inamuro's thermal LBM model

Inamuro et al. (2002) proposed a model for the diffusion system including heat transfer. In their model, there is the simplest distribution function h_i among other thermal models. The LBM equation can be written as:

$$h_i(x + e_i \Delta t, t + \Delta t) - h_i(x, t) = -\frac{1}{\tau_T} \left[h_i(x, t) - h_i^{eq}(x, t) \right], \quad (38)$$

where, τ_T is the dimensionless relaxation parameter.

The equilibrium distribution function (based on D2Q9) for the thermal model can be stated as follows:

$$h_i^{eq}(x, t) = \omega_i T (1 + 3e_i \cdot u) \tag{39}$$

where, T is the temperature.

The diffusion equation corresponding to the thermal model can be expressed as:

$$\frac{\partial T}{\partial t} + u_\alpha \frac{\partial T}{\partial x_\alpha} = \delta \frac{1}{3} \left(\tau_T - \frac{1}{2} \right) \frac{\partial^2 T}{\partial x_\alpha^2} \tag{40}$$

3.3 Phase change based on assumption of Stefan boundary

In the Landau mean-field theory, the phase change is considered as a continuous variable of order parameter. So, the corresponding C-H equation can also be extended to include a phase-change term in the non-isothermal system. The phase change can be identified by calculating the change of phase order parameter. Such a treatment can make the interface be automatically traced based on the change of the phase order parameter. At the same time, the corresponding phase-change latent heat is also considered in the LBM model.

In order to simulate the departure of the vapor bubble from a heated wall and its growth in superheated liquid, two assumptions have to be considered as follows:

1. The vapor inside the bubble is pure and approximately incompressible;
2. The heat transferred from the liquid to the interface is completely used to evaporate the liquid at the interface based on the Stefan boundary, which results in the net increase of bubble volume.

A vapor bubble of volume V'_b is introduced into the superheated liquid. In time interval from t' to $t' + \Delta t'$, the mass transferring into the bubble during the phase change process is expressed as:

$$\int_{V'} \frac{\Delta m}{\Delta t'} dV' = \int \rho_G \frac{dV'_b}{dt} dV' = -\frac{1}{h_{fg}} \int_{S'} \lambda_l \left(\frac{\partial T'}{\partial x'} \right)_b dS' = -\frac{1}{h_{fg}} \int_{V'} \lambda_l \left(\frac{\partial^2 T'}{\partial x'^2} \right)_{V'} dV' \tag{41}$$

where, ρ_G is vapor density, T' is temperature, h_{fg} and λ_l are the latent heat of evaporation and the thermal conductivity, respectively.

Based on phase order parameter, the phase-change is taken into account and expressed as:

$$\dot{\phi} = \frac{\Delta \phi}{\Delta t} = \frac{(\rho_L - \Delta m) - (\rho_G + \Delta m)}{2\Delta t'} - \frac{\rho_L - \rho_G}{2\Delta t'} = -\frac{\Delta m}{\Delta t'} \tag{42}$$

Equation (42) is normalized by the following equations:

$$V_b = \frac{V'_b}{V'_{b0}}, t = \frac{t' U_T}{d_e}, T = \frac{T' - T'_\infty}{T'_b - T'_\infty}, x = \frac{x'}{d_e} \tag{43}$$

where V'_{b0} is the bubble volume at an initial stage, d_e is the equivalent diameter of the bubble, U_T is the terminal rising velocity of the bubble and T'_∞ is the temperature of liquid at the top boundary of the domain. So, the dimensionless form of equation (41) is written as:

$$\rho_G \frac{dV}{dt} = -\frac{\lambda_l (T'_b - T'_\infty)}{h_{fg} U_T d_e} \left(\frac{\partial^2 T}{\partial x^2} \right) \quad (44)$$

By introducing the *Jacob* number $Ja = \frac{1}{h_{fg}} C_{pl} (T'_b - T'_\infty)$ and the *Peclet* number $Pe = \frac{\rho_L U_T d_e C_{pl}}{\lambda_l}$,

Eq. (41) can be expressed as:

$$\frac{dV}{dt} = -\frac{\rho_L}{\rho_G} \frac{Ja}{Pe} \left(\frac{\partial^2 T}{\partial x^2} \right) = \frac{\dot{\phi}}{\rho_L - \rho_G} \quad (45)$$

To include the phase change, the LBM equation (2) when $\phi < 0$ is rewritten as:

$$g_i(x + \bar{e}_i \Delta t, t + \Delta t) - g_i(x, t) = (1 - q) [g_i(x + \bar{e}_i \Delta t, t) - g_i(x, t)] - \frac{1}{\tau_\phi} [g_i(x, t) - g_i^{eq}(x, t)] + \omega_i \dot{\phi} \quad (46)$$

In the LBM Eqs. (37), $\delta \frac{1}{3} \left(\tau_T - \frac{1}{2} \right) = \frac{1}{Pe}$. So when $\phi < 0$, the latent heat term $\frac{\rho_G}{\rho_L (\rho_L - \rho_G)} \cdot \frac{\dot{\phi}}{Ja}$ can be added into the LBM Eqs. (38).

$$h_i(x + \bar{e}_i \Delta t, t + \Delta t) - h_i(x, t) = -\frac{1}{\tau_T} [h_i(x, t) - h_i^{eq}(x, t)] + \omega_i \frac{\rho_G}{\rho_L (\rho_L - \rho_G)} \frac{\dot{\phi}}{Ja} \quad (47)$$

By using the Taylor series expansion and the Chapman-Enskog expansion with respect to Eqs. (46) and (47), the improved governing equations when $\Phi < 0$ can be approximately recovered in the second order form as

$$\frac{\partial \phi}{\partial t} + \nabla \cdot (\phi u) = \theta_M \nabla^2 \mu_\phi - \frac{\rho_L (\rho_L - \rho_G)}{\rho_G} \frac{Ja}{Pe} \left(\frac{\partial^2 T}{\partial x^2} \right) \quad (48)$$

$$\frac{\partial T}{\partial t} + u_\alpha \frac{\partial T}{\partial x_\alpha} = \delta \frac{1}{3} \left(\tau_T - \frac{1}{2} \right) \frac{\partial^2 T}{\partial x_\alpha^2} - \frac{\rho_G}{\rho_L (\rho_L - \rho_G)} \frac{\dot{\phi}}{Ja} \quad (49)$$

To validate the hybrid LBM model including phase change, a phase-change problem with available analytical solution is chosen as a test case, which is the bubble growth in a superheated liquid layer of infinite extent under the condition of no gravity. Initially, a small spherical bubble is rested in the superheated liquid layer. Numerical mesh system has 100*100 numerical cells. A comparison between numerical results and analytical solutions has been carried out and tabulated in Tab.1. It can be discovered that the numerically predicted bubble growth is in good agreement with the Mikic et al. (1970)'s analytical solution, which indicated that the treatment of phase change based on phase order parameter is feasible for the hybrid LBM model.

		Time				
		10	20	30	40	50
Ja=0.0006	Mikic et al. (1970)	0.04375	0.06375	0.07937	0.09324	0.10552
	Present work	0.04339	0.06158	0.0744	0.08519	0.09811
Ja=0.0009	Mikic et al.(1970)	0.06551	0.09243	0.1136	0.1303	0.14406
	Present work	0.06013	0.08691	0.10819	0.12704	0.14412
Ja=0.0012	Mikic et al.(1970)	0.08736	0.12382	0.15126	0.17416	0.19613
	Present work	0.08197	0.11746	0.14672	0.17236	0.19579

Table 1. Comparison of the calculated radius of bubble growth with the Mikic’s solution (Pe=3000)

Accounting for the buoyancy force as stated in the reference (Zheng et al., 2006), we define the Eo, M and Re as follows:

$$Eo = \frac{g(\rho_H - \rho_L)d^2}{\sigma}, M = \frac{g(\rho_H - \rho_L)\mu_H^4}{\rho_H^2\sigma^3}, Re = \frac{\rho_H V_T d}{\mu_H}$$

The bubble volume is calculated by $V'_b(t) = \frac{\sum_{\phi < 0} \phi(t)}{\sum_{\phi < 0} \phi(t_0)}$ and the growth rate of bubble

volume is calculated by $\dot{V}'_b = [V'_b(t + \Delta t) - V'_b(t)] / \Delta t$.

3.4 Numerical simulation of vapor bubble growth on and departure from a superheated wall

3.4.1 The Briant’s treatment of partial wetting boundary

The Briant’s treatment of the partial wetting boundary is introduced into the hybrid LBM model elaborated above. The details of this treatment is available in the literature (Biant et al., 2002). Adjustment aroused by the wetting boundary is considered as follows:

1. A little order parameter non-conservation induced by the distribution functions at inflow and outflow on the wetting boundary is counted and apportioned to every node occupied by the bubble.
2. The surface tension forces between the wall and fluids are adjusted to guarantee the vapor bubble to be able to expand and depart in integrality on the wetting boundary like action of an actual vapor bubble in practical processes. Therefore, according to the

Young’s law ($\cos\theta_w = \frac{\sigma_{SG} - \sigma_{SL}}{\sigma_{LG}}$), the order parameter Φ_G is set as -90 or smaller in this

work. The contact angle is adjusted in relative to the corresponding Φ_L . The comparison of resulting effects is schematically shown in Fig.6.

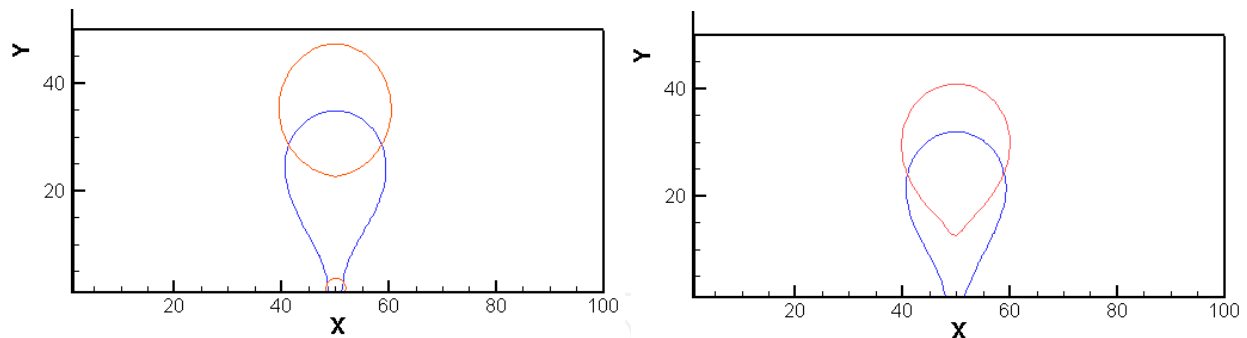


Fig. 6. Effect of different adsorb ability (left: $\Phi_G < -90$; right: $\Phi_G > -90$) on wetting boundary
The corresponding properties are taken as follows;

$$\rho_L = 1000, \rho_G = 1, \Gamma = 650, Pecllet = 3000, Eo = 72, M = 3.44.$$

The mesh of the domain is generated as 100×50 . A spherical bubble with radius of 3 is located in (50, 2). The flow field is surrounded with one partial wetting boundary (bottom boundary), one extrapolated-boundary (top boundary) and two stationary walls (left and right boundaries). The initial thermal boundary layer thickness is calculated from the correlation (Han et al., 1965):

$$\delta = \frac{3}{2} \frac{(T_w - T_\infty) R_c}{T_w - T_{sat} [1 - (2\sigma / R_c \rho_v L)]}$$

where, R_c is the initial bubble radius.

As far as the bubble departure diameter is concerned, different physical parameters, such as body force, surface tension force, and partial wetting boundary and *Jacob* number are considered and investigated. The most widely used correlation for the bubble departure diameter on the heated surface was proposed by Fritz (1935), in which the bubble departure was determined by a balance between the buoyancy and surface tension force acting normal to the solid surface. Based on the experimental measurement of the departure diameter over a pressure range, and observation of the influence of the bubble growth rate on the departure diameter, Staniszewski (1959) modified the Fritz (1935) equation to obtain the departure diameter correlation as follows:

$$D_d = 0.0071 \beta \left(\frac{2\sigma}{g\Delta\rho} \right)^{\frac{1}{2}} \left(1 + 34.3 \frac{\partial D}{\partial t} \right)$$

where $\frac{\partial D}{\partial t}$ denotes the bubble growth rate.

Using the present method, the effect of physical parameters on the departure diameter is investigated. The calculated departure diameter for different gravity forces and surface tension forces are regressed to functions as $D \propto g^{-0.472}$ and $D \propto \sigma^{0.5}$. The result is in very good agreement with the Fritz (1935) relation. The calculated correlation of departure diameter and the *Jacob* number is a regressed function of $D \propto Jacob$. Because the *Jacob* number is a dominant factor of the bubble growth rate, the result shows indirectly the correlation between the departure diameter and the bubble growth as predicted by

Staniszewski (1959)'s correlation. The departure diameter changes with the adjustment of Φ_L . Because the contact angle is determined by Φ_L and Φ_G , the adjustment of Φ_L can change the contact angle and influence the bubble departure diameter. The precise quantitative relation between contact angle and departure diameter is still under investigation.

3.4.2 Propagation of flow field

Fig.7 presents the evolution of flow field accompanying with the corresponding stream traces. It can be seen from these figures how the bubble growth and departure affect the flow field. In the early stage, due to the bubble growth or expanding on the wetting boundary, two vortices are formed on both sides of the bubble. The vortices (including shape and intensity) are enforced to develop with the bubble further growing up. With the process continuing, the change of shape induces the vortex breaking up into twin-vortex. With the bubble starting with departure, the twin-vortices on both sides incorporate into a single vortex and rise up with the bubble. In the late stage, the vortices further strengthen their scopes and intensity and rise up accompanying with the bubble departure.

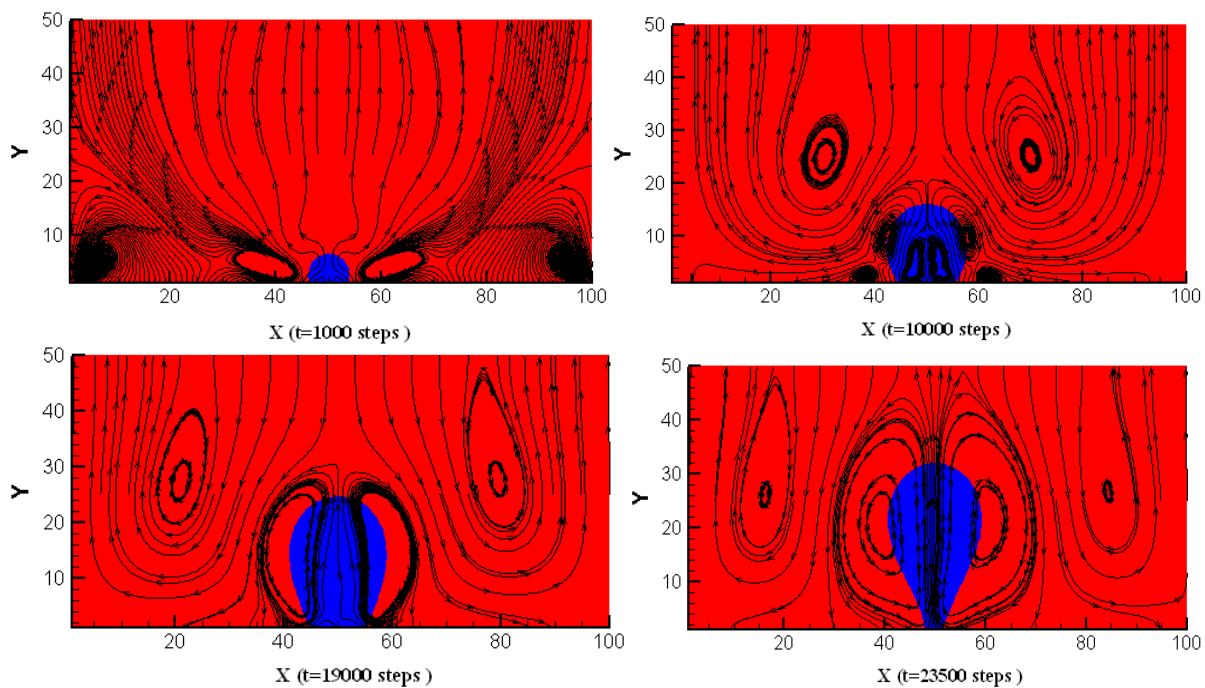


Fig. 7. Propagation of flow field

3.4.3 Propagation of temperature field

The evolution of temperature field is depicted in Fig.8. The effects of the bubble growth and departure on the temperature field around the bubble are clearly seen. In the early stage, due to its small volume, the bubble phase-change is dependent on the heat transfer in the micro layer and macro layer both. With growing up of the bubble, the contribution of heat transfer in the macro layer is gradually weakened. In the process of the bubble departure, the forced convection induced by the ascending bubble greatly affects the temperature field. The disturbance to the temperature field, in return, influences the bubble growth and departure to some extent.

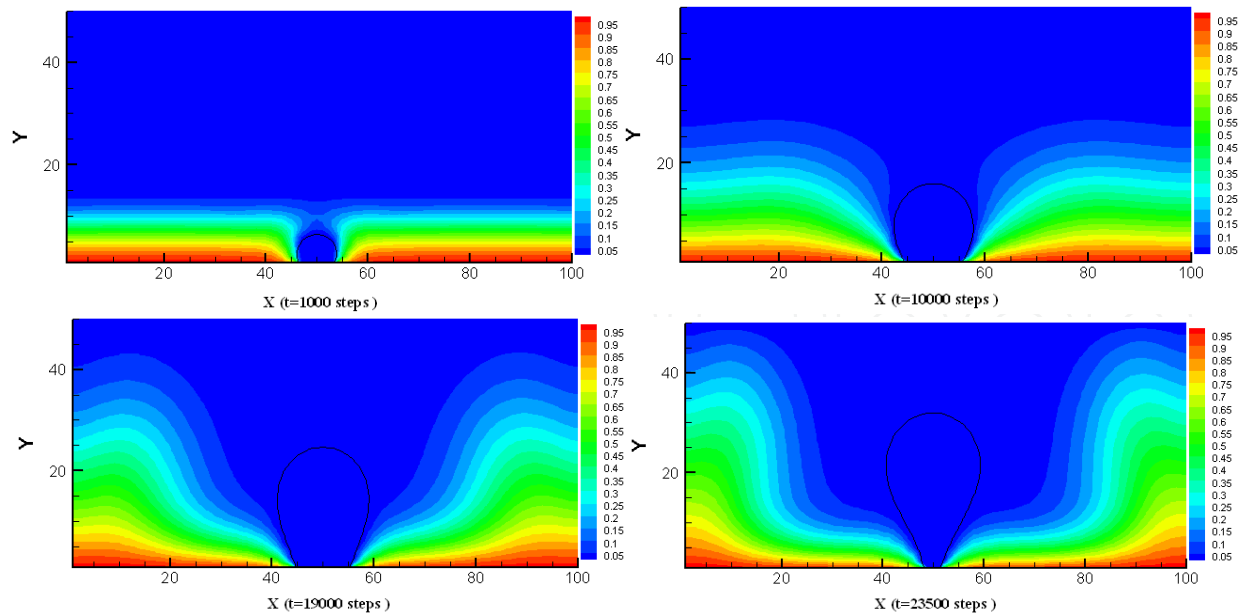


Fig. 8. Propagation of temperature field

3.4.4 Characteristics of two bubbles growth on and departure from the wall

Based on the LBM elaborated above, two bubbles coalescence dynamics on a horizontal surface are also investigated. The simulation focuses on the effect of twin-bubble distance (*dist*) on the bubble growth, coalescence and departure. The result is shown in Fig.9 and the bubble diameter is calculated from the summation of the two bubbles' volume. It is easily

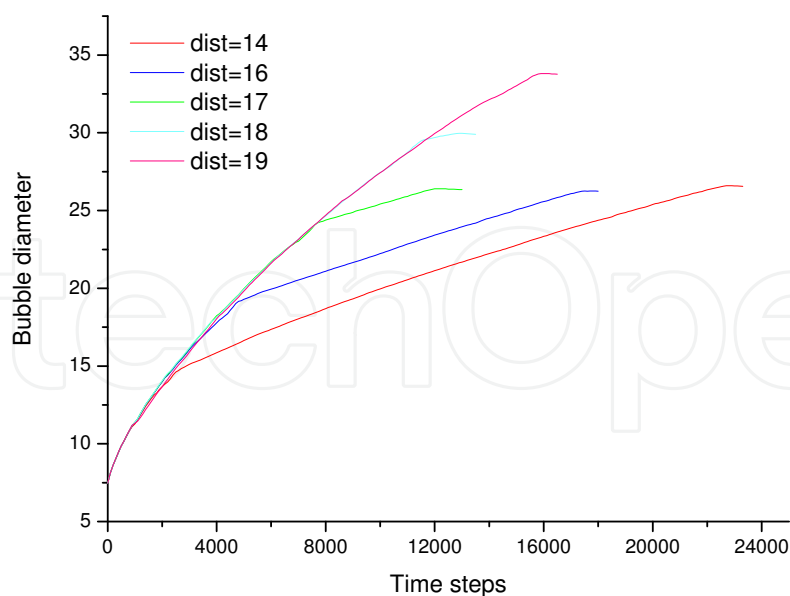


Fig. 9. Bubble growth and departure in different coalescence conditions

found that the final result is closely related to twin-bubble distance. With the distance increasing, the coalescence is delayed and the departure time is shortened to some extent. But the diameter of bubble departure does not change with the coalescence of bubbles of

different distance, like $dist=14, 16,$ and 17 . With the distance increasing further, the effect of coalescence on bubble growth rate disappears except the diameter of bubble departure is becoming larger, (see cases with $dist=18$ and 19). When the bubble departs from the surface in its integrality, the bubble growth rate tends to become zero, i.e.; the growth ceases.

Figs.10 and 11 show the evolving process of flow and temperature field, respectively. From Fig. 10, it is seen that before the bubble coalescence, two vortices are forming on the outward side of the twin-bubbles, respectively. With growing up and coalescence of the bubbles, both vortices are strengthened. They both are split into one clockwise vortex and one anti-clockwise vortex with the bubbles further growing up. After the two bubbles coalesce, we see firstly four bubbles with 2 of them locating on one side of bubble and the other 2 on the other side. Then the merged large bubble further grows up, until it departs from the wall. Vortices on the same side of the merged bubble are developing further and converge into one. Afterwards, we see one bubble ascending in the liquid with 2 vortices locating on right and left side respectively. Fig.11 shows the related temperature field. It is easily found that the forced convection directly influences the temperature field especially after bubble coalesces and departs.

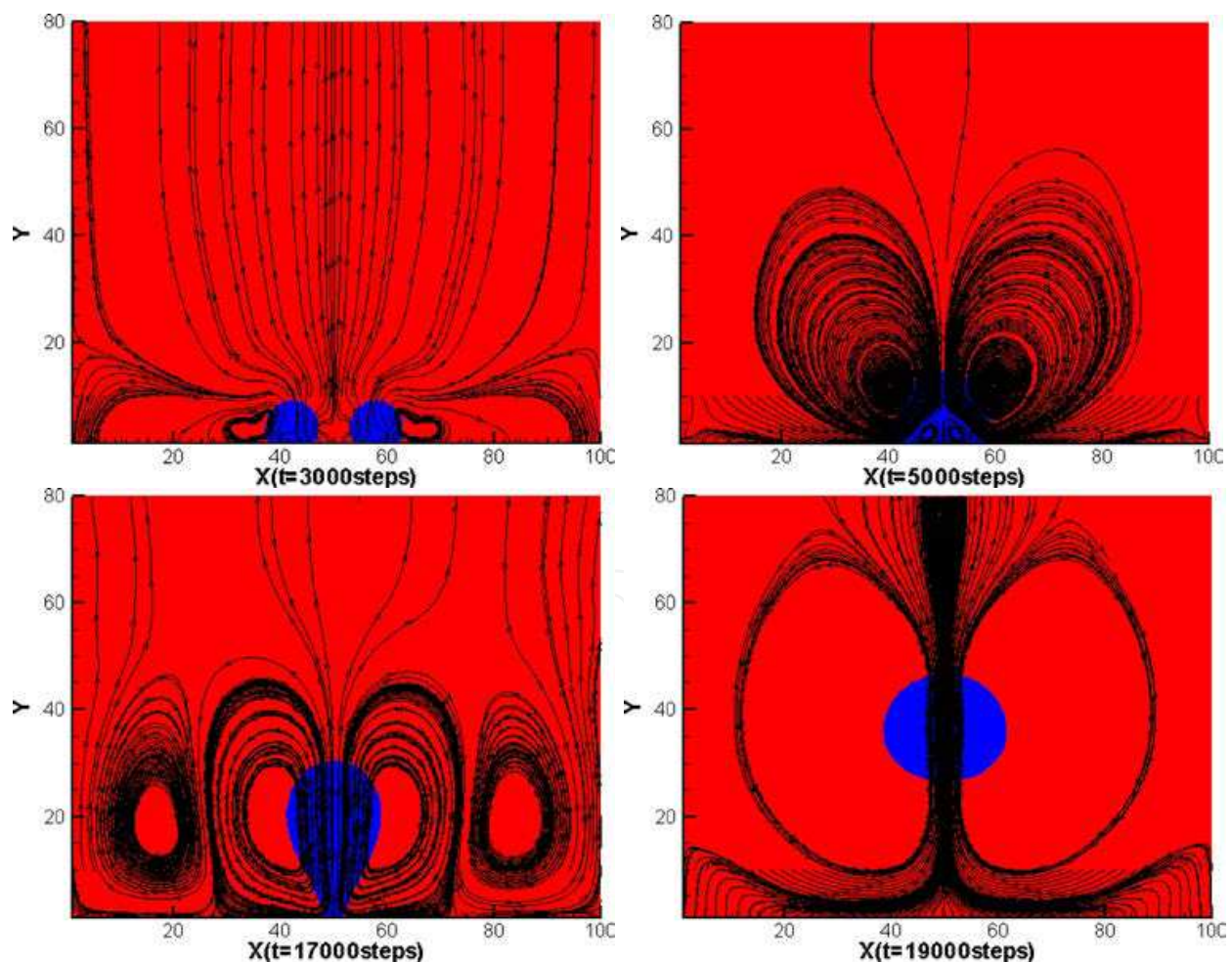


Fig. 10. Propagation of flow field

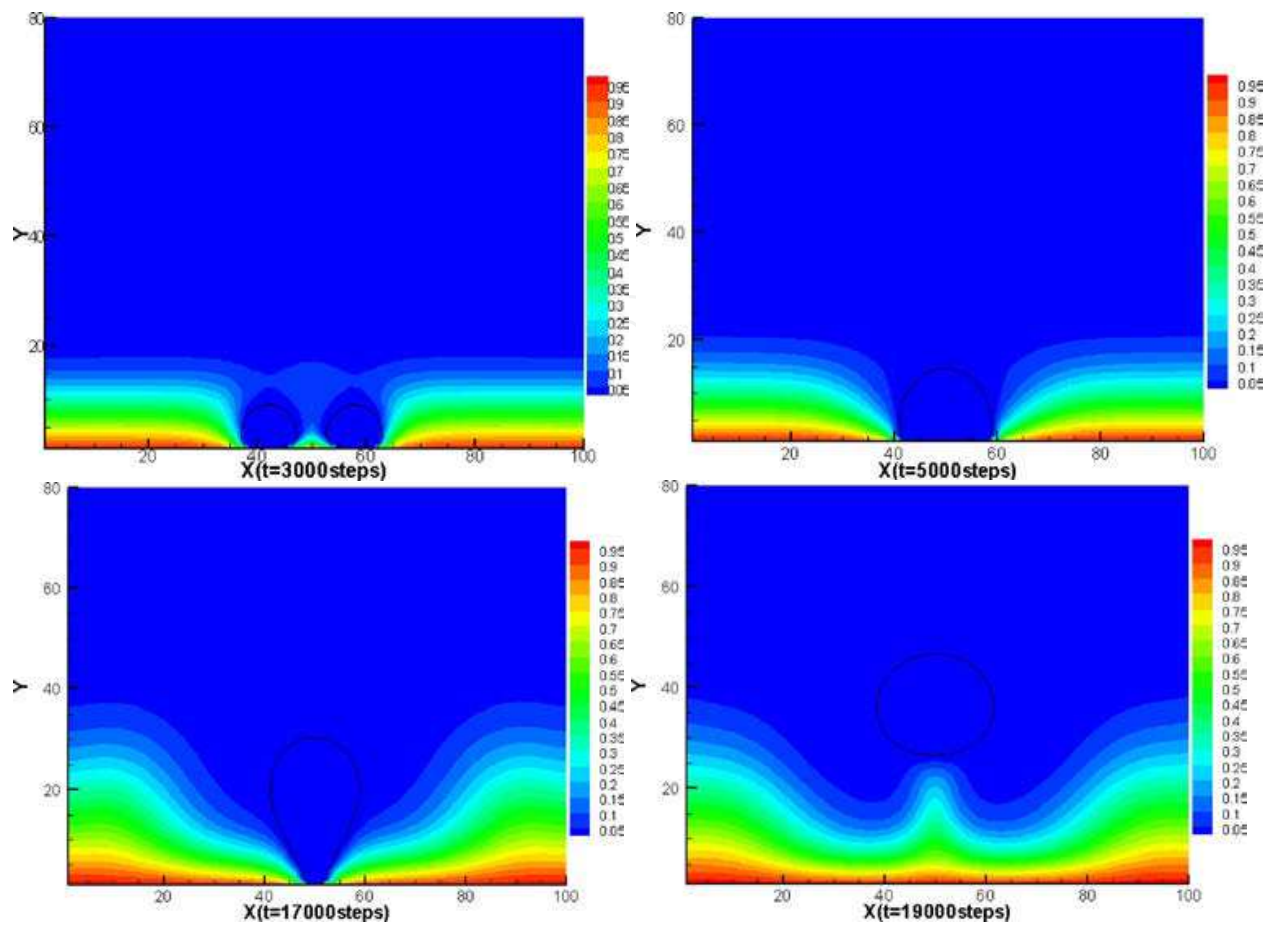


Fig. 11. Propagation of temperature field

4. Concluding remarks

In this chapter we reviewed the current state-of-the-art and recent advances of LBM through case studies. We presented firstly an improved LBM for modeling the mass transport in multi-component systems, which was used to simulate the mixing process in a rotating packed bed with a serial competitive reaction ($A+B \rightarrow R$, $B+R \rightarrow S$; A , B , R , and S denote different components.) occurring therein. The obtained results provide some guidance for further studying the forced mass-transfer in and for the design of the real rotating packed-bed in industries. Secondly, with a purpose to simulate phase change process, the LBM multiphase model being able to handle a large ratio of density between phases is combined with the LBM thermal model to form a hybrid LB model. By introducing the Briant's treatment to partial wetting boundary, this hybrid model was used to investigate growth and departure of a single bubble, and coalescence of twin-bubbles, on (or from) a heated horizontal surface. Numerical results exhibited correct parametric dependence of the departure diameter as compared to the experimental correlation available in the literatures. The capability and suitability of this hybrid LB model for modeling complex fluid and heat/mass transfer systems are thus demonstrated. Due to its terseness advantage in the treatment of complex boundary, our future work will further extend this hybrid model to simulate multiphase and/or multi-component flows in complex systems, such as in porous media of complex micro-pore structures encountered fuel cell (battery) realms.

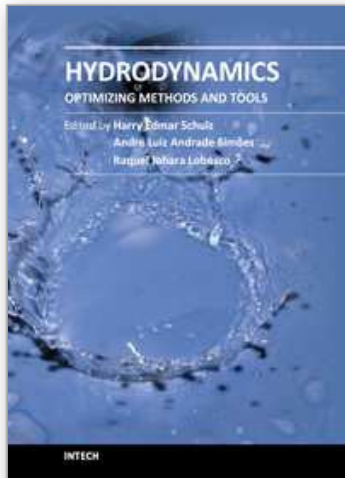
5. Acknowledgement

Financial support received partially from the CAS "100 Talent" Program (FJ) is gratefully acknowledged.

6. References

- Alexander, F. J., Chen, S., & Sterling J. D. (1993). Lattice Boltzmann thermo hydrodynamics [J]. *Phys. Rev E*, 47: 2249-2252
- Bhaga, D. & Weber, M. E. (1981). Bubbles in viscous liquid: shapes, wakes and velocities, *J. Fluid Mech.* Vol.105, pp.61~85.
- Bartoloni, A., Batisita, C., & Cabasino, S. (1993). Lbr Simulations of Rayleigh-Benard convection on the Ape100 parallel process [J]. *Int.J.Mod.Phys, C4*: 993-1006.
- Briant, A.J., Papatzacos, P., & Yeomans, J.M. (2002). Lattice Boltzmann simulations of contact line motion in a liquid-gas system, *Philos.Trans.Roy.Soc.London A* 360: 485-495
- Chen, H., Teixeira, C., & Molving K. (1997). Digital Physics Approach to computational fluid dynamics: some basic theoretical features [J]. *Int. J. Mod. Phys*, 8: 675-684.
- Cao, J. & Christensen, R. N. (2000). Analysis of moving boundary problem for bubble collapse in binary solutions, *Numerical Heat Transfer. Part A, Vol.38*. pp.681~699.
- Dong, Z., Li, W., & Song, Y. (2009). Lattice Boltzmann simulation of growth and deformation for a rising vapor bubble through superheated liquid, *Numerical Heat Transfer. Part A*, 55:381-400.
- Fritz, W. & Maximun. (1935). volume of vapor bubbles, *Physik Zeitschr.* 36 : 379-384
- Fujita, Y. & Bai, Q. (1998). Numerical simulation of the growth for an isolated bubble in nucleate boiling, *Proceedings of 11th IHTC. Kyongiu, Korea, August 23-28, Vol.2*. pp. 437~442.
- Frish, U., Hasslacher, B., & Pomeau, Y. (1986). Lattice-Gas Automata for the Navier-Stokes equation [J]. *Phys.Rev. Lett*, 56 (14): 1505-1508.
- He, X., Chen, S., & Zhang, R. (1999). A lattice Boltzmann scheme for incompressible multiphase flow and its application in simulation of Rayleigh-Taylor instability. *J.Comput.Phys.* 152 (2) 642-663.
- Han, C. & Griffith, P. (1965). The mechanism of heat transfer in nucleate pool boiling. *Int.J.Heat MassTransfer* 8, 887-914.
- Han, Y. & Seiichi, K.Y.O. (2001). Direct calculation of bubble growth, departure, and rise in nucleate pool boiling, *Int. J. of Multiphase Flow*. Vol.27, pp.277~298.
- Hua, J. & Lou, J. (2007). Numerical simulation of bubble rising in viscous liquid, *J. Comp. Phys.* Vol.222, pp.769~795.
- Inamuro, T., Ogata, T., Tajima, S., & Konishi, N. (2004). A Lattice Boltzmann method for incompressible two-phase flows with large density differences. *J. Comp. Phys.* Vol.198, pp.628~644.
- Inamuro, T., Yoshino, M., Inoue, H, Mizuno, R., & Ogino F. (2002). A lattice Boltzmann method for a binary miscible fluid mixture and its application to a heat-transfer problem [J]. *J. Comp. Phys*, 179: 201-215.
- Luo, X., Ni, M., Ying, A., & Abdou, M. (2005). Numerical modeling for multiphase incompressible flow with phase change, *Numerical Heat Transfer. Part.B. Vol.48*. pp.425~444
- Liu, J. (2000). Study on micro-mixing and synthesis of nanometer particle of strontium carbonate by mixing two section of solutions in Rotating Packed Bed [D]. Beijing: Beijing University of Chemical Technology.

- Li, W. & Yan, Y. (2002). An alternating dependent variables(ADV) method for treating slip boundary conditions of free surface flows with heat and mass transfer, *Numerical Heat Transfer (An International Journal of Computation and Methodology)*, Part B, Vol. 41, No.2, pp. 165~189.
- Li, W. & Yan, Y.(2002). A direct-predictor method for solving terminal shape of a gas bubble rising through a quiescent liquid, *Numerical Heat Transfer (An International Journal of Computation and Methodology)*, Part B, Vol. 42, No.1, pp. 55~71.
- Lee, T. & Lin, C. (2005). A stable discretization of the lattice Boltzmann equation for simulation of incompressible two-phase flows at high density ratio, *J.Comput.Phys.*206:16-47.
- Mukherjee, A. & Kandlikar, S.G.(2007). Numerical study of single bubbles with dynamic contact angle during nucleate pool boiling, *Int. J. Heat and Mass Transfer*, 50 : 127-138.
- Mikic, B.B., Rohsenow, W.M., & Griffith, P.(1970). On bubble growth rate, *Int. J. Heat Mass Transfer* 13, 657-666 .
- Plesset, M.S. & Zwick, S.A.(1953). The growth of vapor bubble in superheated liquids, *J. Applied Physics*.Vol.25.No.4.pp.293~500.
- Rothman, D.H. & Keller, J.M.(1998). Immiscible cellular-automaton fluid, *J. Statist. Phys.* 52. pp.1119~1127.
- Staniszewski, B.E. (1959). Nucleate boiling bubble growth and departure, MIT Tech..Rep.No.16, Cambridge, MA.
- Soe, M., Vahala, G., Pavlo, P., Vahala, L., & Chen, H. (1998).Thermal lattice Boltzmann simulations of variable Prandtl number turbulent flows [J]. *Phys. Rev E*, 57(4): 4227-4237.
- Shan, X. (1997). Simulation of Rayleigh-Benard convection using a lattice Boltzmann method [J]. *Phys.Rev.E*, 55: 2780-2788
- Son, G. & Dhir, V.K. (1998). Numerical simulation of a single bubble during particle nucleate boiling on a horizontal surface, *Proceedings of 11th IHTC. Kyongju, Korea, August 23-28, Vol.2. pp.533~538.*
- Shan, X. & Chen, H. (1993). Lattice Boltzmann model for simulating flows with multiple phases and components, *Phys. Rev. E*47(3).pp.1815~1819.
- Swift, M.R., Orlandini, E., Osborn,W.R., Yeomeans, J.M. (1996). Lattice Boltzmann simulations of liquid-gas and binary fluid systems, *Phys.Rev. E*54.pp.5041~5052.
- Tomiyama, A., Sou, A.; Minagawa, H., & Sakaguchi, T. (1993). Numerical analysis of a single bubble by VOF method, *JSME Int J. Series B. Vol.36.No.1.*
- Vahala, G., Pavlo, P., Vahala, L., & Martys, N. S. (1998). Thermal lattice-Boltzmann models (TLBM) for compressible flows[J]. *Int. J. Mod. Phys C*, 9: 1247-1261.
- Vahala, L., Wah, D., Vahala, G., Carter, J., & Pavlo, P. (2000).Thermal lattice Boltzmann simulation for multispecies fluid equilibration[J]. *Phys. Rev E*, 62: 507-516.
- Wittke, D.D. & Chao, T.B. (1967). Collapse of vapour bubbles with translatory motion, *J. Heat Transfer. Vol.89. pp.17~24.*
- Yan, Y., & Li, W. (2006). Numerical modelling of a vapors bubble growth in uniformly superheated liquid, *Int J. of Numerical Methods for Heat & Fluid Flow*, Vol.16. No.7. pp.764~778.
- Zheng, H.W., Shu, C., & Chew, Y.T.(2006). A Lattice Boltzmann for multiphase flows with large density ratio, *J. Comput. Phys. Vol.218. pp.353~371.*



Hydrodynamics - Optimizing Methods and Tools

Edited by Prof. Harry Schulz

ISBN 978-953-307-712-3

Hard cover, 420 pages

Publisher InTech

Published online 26, October, 2011

Published in print edition October, 2011

The constant evolution of the calculation capacity of the modern computers implies in a permanent effort to adjust the existing numerical codes, or to create new codes following new points of view, aiming to adequately simulate fluid flows and the related transport of physical properties. Additionally, the continuous improving of laboratory devices and equipment, which allow to record and measure fluid flows with a higher degree of details, induces to elaborate specific experiments, in order to shed light in unsolved aspects of the phenomena related to these flows. This volume presents conclusions about different aspects of calculated and observed flows, discussing the tools used in the analyses. It contains eighteen chapters, organized in four sections: 1) Smoothed Spheres, 2) Models and Codes in Fluid Dynamics, 3) Complex Hydraulic Engineering Applications, 4) Hydrodynamics and Heat/Mass Transfer. The chapters present results directed to the optimization of the methods and tools of Hydrodynamics.

How to reference

In order to correctly reference this scholarly work, feel free to copy and paste the following:

Zhiqiang Dong, Weizhong Li, Yongchen Song and Fangming Jiang (2011). Lattice Boltzmann Computations of Transport Processes in Complex Hydrodynamics Systems, *Hydrodynamics - Optimizing Methods and Tools*, Prof. Harry Schulz (Ed.), ISBN: 978-953-307-712-3, InTech, Available from:
<http://www.intechopen.com/books/hydrodynamics-optimizing-methods-and-tools/lattice-boltzmann-computations-of-transport-processes-in-complex-hydrodynamics-systems>

INTECH
open science | open minds

InTech Europe

University Campus STeP Ri
Slavka Krautzeka 83/A
51000 Rijeka, Croatia
Phone: +385 (51) 770 447
Fax: +385 (51) 686 166
www.intechopen.com

InTech China

Unit 405, Office Block, Hotel Equatorial Shanghai
No.65, Yan An Road (West), Shanghai, 200040, China
中国上海市延安西路65号上海国际贵都大饭店办公楼405单元
Phone: +86-21-62489820
Fax: +86-21-62489821

© 2011 The Author(s). Licensee IntechOpen. This is an open access article distributed under the terms of the [Creative Commons Attribution 3.0 License](#), which permits unrestricted use, distribution, and reproduction in any medium, provided the original work is properly cited.

IntechOpen

IntechOpen